

Article

# Beachrock as a Paleoshoreline Indicator: Example from Wadi Al-Hamd, South Al-Wajh, Saudi Arabia

Ammar A. Mannaa<sup>1</sup>, Rabea A. Haredy<sup>1</sup> and Ibrahim M. Ghandour<sup>1,2,\*</sup> 

<sup>1</sup> Marine Geology Department, Faculty of Marine Science, King Abdulaziz University, P.O. Box 80200, Jeddah 21589, Saudi Arabia; amanna@kau.edu.sa (A.A.M.); rhardy@kau.edu.sa (R.A.H.)

<sup>2</sup> Geology Department, Faculty of Science, Tanta University, Tanta 31527, Egypt

\* Correspondence: ighandour@kau.edu.sa

**Abstract:** The present study concerns the Holocene inland beachrocks that are exposed in the Red Sea coastal plain at the mouth of Wadi Al-Hamd, South Al-Wajh City, Saudi Arabia, and their utility as an indicator for Holocene climate and sea level changes. In addition, the framework composition, and carbon and oxygen isotopic data, are employed to interpret the origin of their cement. The beachrock consists mainly of gravel and coarse-grained terrigenous sediments dominated by lithic fragments of volcanic rocks, cherts and rare limestones along with quartz, feldspars and traces of amphiboles and heavy minerals. In addition, rare skeletal remains dominated by coralline algae, benthic foraminifera and mollusca remains are recognized. The allochems are cemented by high Mg-calcite (HMC) formed mainly in the intertidal zone under active marine phreatic conditions. The cement takes the form of isopachous to anisopachous rinds of bladed crystals, micritic rim non-selectively surrounding siliciclastic and skeletal remains, and pore-filling micrite. Pore-filling micrite cement occasionally displays a meniscus fabric, suggesting a vadose environment. The  $\delta^{18}\text{O}$  and  $\delta^{13}\text{C}$  values of carbonate cement range from  $-0.35\text{‰}$  to  $1\text{‰}$  (mean  $0.25\text{‰}$ ) and  $-0.09\text{‰}$  to  $3.03\text{‰}$  (mean  $1.85\text{‰}$ ), respectively, which are compatible with precipitation from marine waters. The slight depletion in  $\delta^{18}\text{O}$  and  $\delta^{13}\text{C}$  values in the proximal sample may suggest a slight meteoric contribution.

**Keywords:** beachrocks; paleoshoreline; Holocene sea-level and climate changes; Wadi Al-Hamd; Red Sea



**Citation:** Mannaa, A.A.; Haredy, R.A.; Ghandour, I.M. Beachrock as a Paleoshoreline Indicator: Example from Wadi Al-Hamd, South Al-Wajh, Saudi Arabia. *J. Mar. Sci. Eng.* **2021**, *9*, 984. <https://doi.org/10.3390/jmse9090984>

Academic Editor: Gemma Aiello

Received: 13 August 2021  
Accepted: 5 September 2021  
Published: 8 September 2021

**Publisher's Note:** MDPI stays neutral with regard to jurisdictional claims in published maps and institutional affiliations.



**Copyright:** © 2021 by the authors. Licensee MDPI, Basel, Switzerland. This article is an open access article distributed under the terms and conditions of the Creative Commons Attribution (CC BY) license (<https://creativecommons.org/licenses/by/4.0/>).

## 1. Introduction

The development of the Red Sea coastal zone is an important axis in the new economic vision of Saudi Arabia. Development plans and the forecasting of future changes along the Red Sea coastal area should take into account Holocene sea level and climate changes. The impact of Holocene sea level and climate changes, and their influence on the depositional and erosional processes of the coastal zone, is a pertinent topic in geological and archaeological research and coastal zone development plans [1]. The Holocene sea level rose rapidly from the Last Glacial Maximum (LGM) until 6–7 ka ago, when most of the continental ice sheets melted [2]. Correspondingly, the climate was more humid during that time, and turned extremely arid starting from about 5 ka ago [3]. During the humid early and middle Holocene, floods may have been more frequent than they are today, and perhaps more capable of carrying a larger coarse sediment load.

Several proxies have been utilized worldwide to infer Holocene climate and sea level changes. These proxies include shoreline shifts and subsequent vertical variations in sedimentary facies [4–7], temporal variations of microfossils [8,9], beachrocks, marine notches and raised coral reefs [10–14]. Recent descriptions of coastal sedimentology of the tropics and warm temperate zones render beachrocks as potentially useful indicators of sea level and climatic changes and former paleoshoreline positions [13,15,16]. Beachrocks are an outstanding sea level proxy since they hold information on not only the vertical but also the lateral evolution of the shoreline [17,18].

Beachrocks are carbonate cemented littoral sediments of different compositions (terigenous, biogenic and anthropogenic) and grain sizes (sand to gravel) typically found within the intertidal zones and, rarely, in supratidal and lower subtidal zones along low latitude coastlines ([15,19–22]. The cementation process is accomplished under various climatic conditions by supersaturation of interstitial water, intensive evaporation, mixing of marine and meteoric waters [23], CO<sub>2</sub> degassing of intertidal groundwater [24] and by the aid of biological activities [25]. The texture, microfabrics and mineralogy of carbonate cements provide information about the formation mechanisms and environmental conditions of cementation.

Beachrocks of different composition and grain size are distributed intermittently along the Saudi Red Sea and the Gulf of Aqaba coasts. They consist mainly of gravel- and sand-sized siliciclastic grains and/or calcareous skeletal remains, cemented by aragonite and/or high Mg-calcite (HMC) and, rarely, low Mg-calcite [22,26–29]. The beachrocks along the Saudi Red Sea and the Gulf of Aqaba coasts have received little attention compared to the Egyptian and Jordanian coasts ([19,25,30–32]. An interesting, not previously documented beachrock crops out far inland, 1.1 km from the recent shoreline at the mouth of Wadi Al-Hamd, 50 km south of Al-Wajh City, at latitude N 25° 57.737' and longitude E 36° 42.721' (Figure 1). This implies an in-situ cementation at the intertidal level within the sedimentary pile after deposition. The present study aims to interpret the depositional setting of these beachrocks and their relationship to Holocene climate and sea level changes. The study will further determine the cement’s mineralogical composition and microfabric in an attempt to gain information about the source of cement.

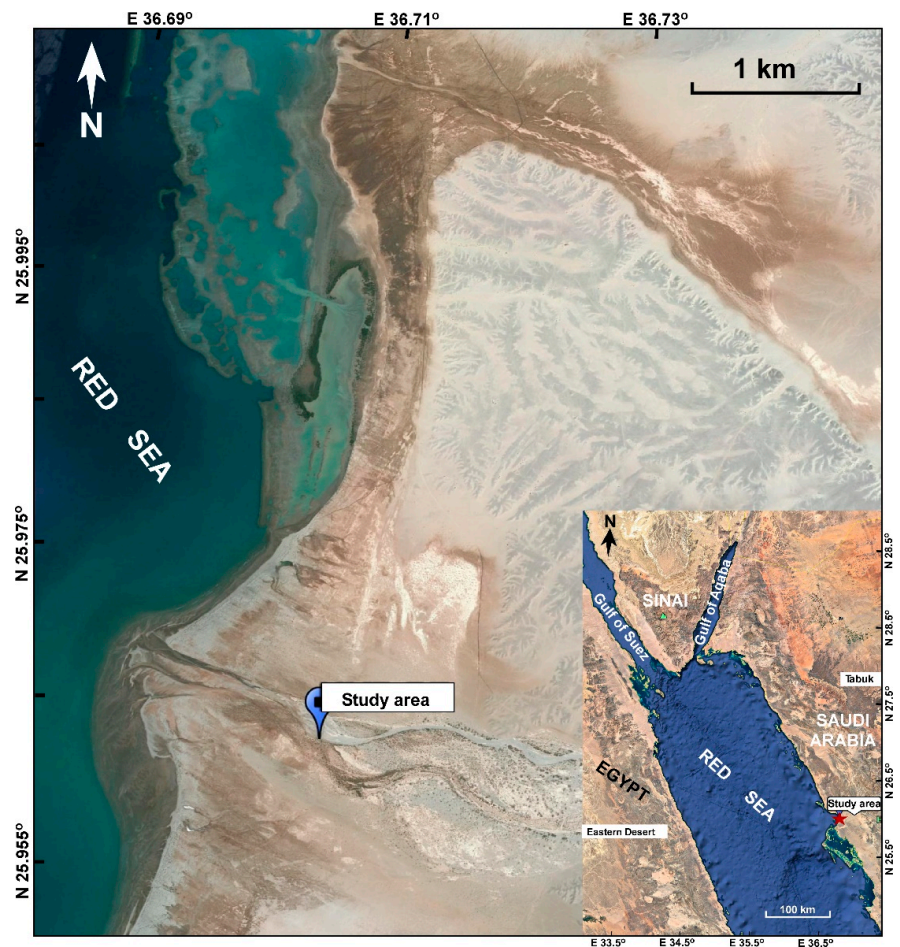


**Figure 1.** Landsat image shows the area of study and the location of the beachrock exposure at the mouth of Wadi Al-Hamd.

## 2. Area of Study

The area of study is located at the mouth of Wadi Al-Hamd, northern Red Sea, about 55 km south of Al Wajh City, Saudi Arabia, at latitude N 25° 57.737' and longitude E 036° 42.721' (Figure 1). Wadi Al-Hamd is one of the largest wadis shedding the Arabian Shield in northern Saudi Arabia. It extends from mountain scarp near Al-Medina City, flows inland to NW and discharges sediments and freshwaters into the Red Sea. For most of the year, Wadi Al-Hamd is extremely dry; however, in the winter (October and March), it temporarily activates during episodic major flood seasons in the form of short-duration showers generally associated with thunderstorms. The climate in the area is identified by its arid desert; dry, hot summers with maximum daily temperatures that range from 20 °C to 35 °C in January and up to 48 °C in July. The precipitation rate ranges from 0.5 to 116 mm/year, whereas the evaporation rate is high, up to 2 m<sup>3</sup>/year or slightly more [33]. The prevailing winds are from the NNW to SSE over the entire year with speed varying from 2 to 10 m/s [33]. Wave heights of up to 2.5 m and, rarely, up to 4 m are generated by the strong onshore-directed winds. The area has a semidiurnal microtidal regime, with a spring and neap tidal range of 0.7 m and 0.5 m, respectively. Although relatively weak, the strength of flood tidal currents is stronger than the almost insignificant ebb currents. From an aerial view, the clastic-dominated coast of Wadi Al-Hamd is linear to slightly arched, projecting itself seaward at the mouth of the wadi. It is an asymmetric lobate delta, flanked to the north by a narrow strandplain with a relatively steep foreshore profile and a wide, low gradient intertidal flat to the south, separated by a low relief beach ridge [5,34]. Sabkhas and coastal sand dunes occupy the flood plain, while the channel is barred seaward by a low relief beach ridge with back-barrier swale separating the channel from the sea. The strandplain to the north contains a series of sand bars and a runnel system running parallel to slightly slanted to the shoreline [5]. A fringing reef and mangrove tickets occur to the north and away from the influence of wadi sedimentation. The nearshore sediment composition is dominated by detrital siliciclastic minerals, which are dominated by plagioclase with subordinate feldspars, amphiboles and traces of heavy minerals [35].

The coastal plain of the area south Al-Wajh is covered by Quaternary siliciclastic sediments (Figure 2). The sediments are derived mainly from the Precambrian Basement Complex of the Arabian shield and the Cenozoic volcanic and sedimentary rocks. These rocks crop out in the surrounding area and along the axis of the wadi from the catchment area near Al-Medina City to the downstream area. The downstream area of Wadi Al Hamd is covered by Quaternary alluvial terraces in the lower part consisting of consolidated, very coarse sediments of Pleistocene age, overlain by Recent unconsolidated gravel and sand [35–37].

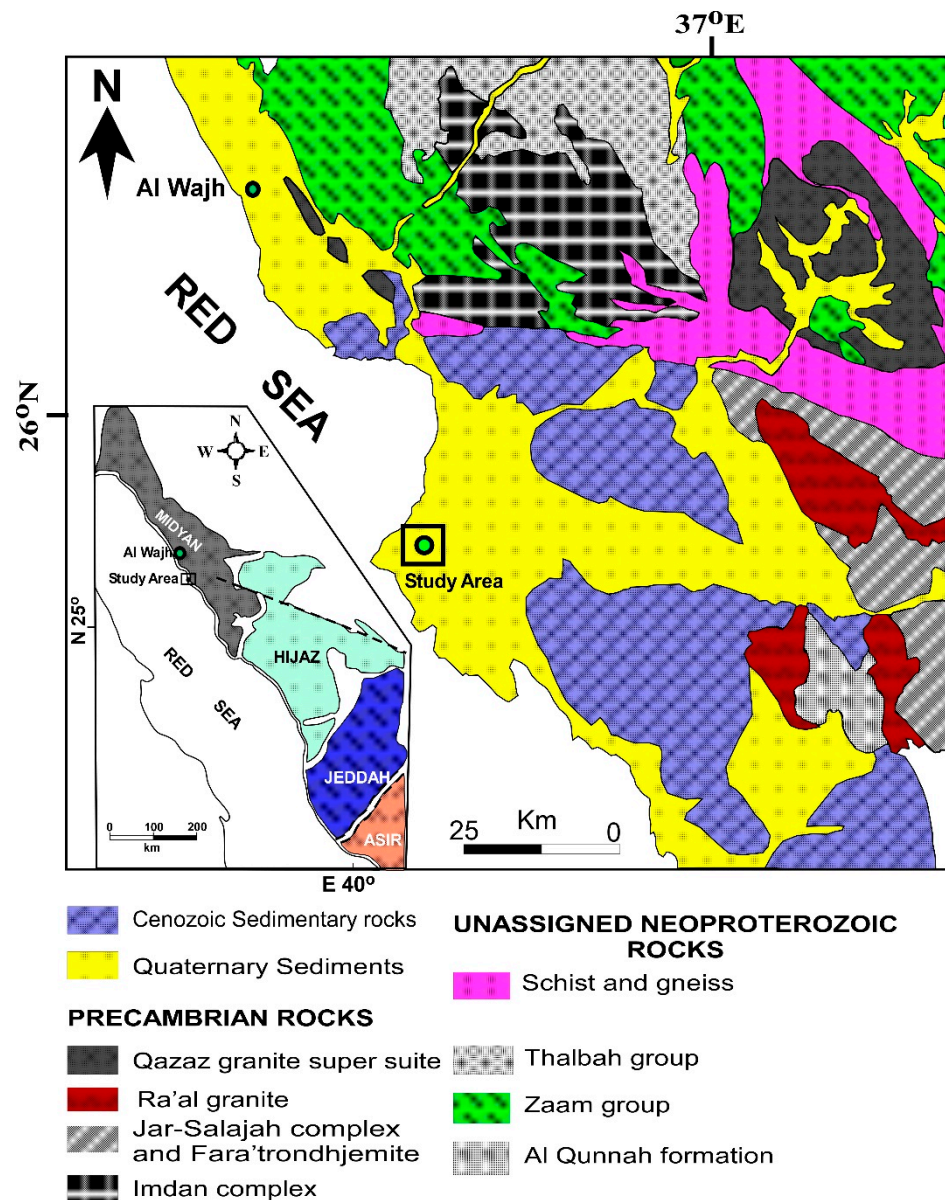
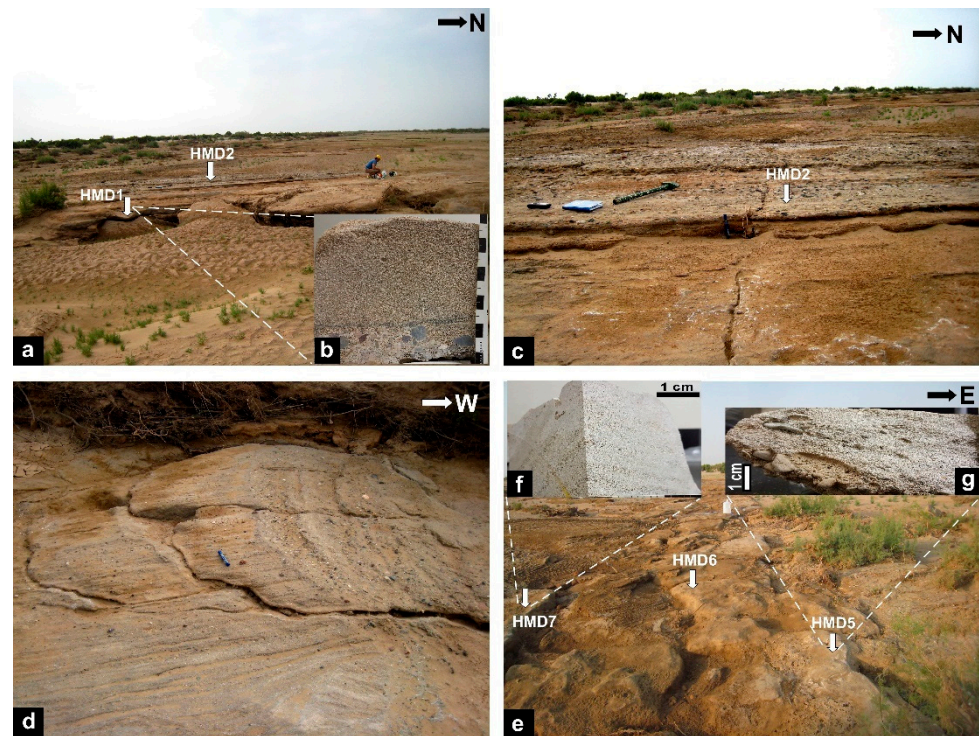


Figure 2. Simplified geologic map of the area of study (adapted from [37]).

### 3. Materials and Methods

Five samples were collected from the beachrock exposure at the mouth of Wadi Al-Hamd (Figure 3). Thin sections were prepared following traditional methods at the Petrology Lab, Faculty of Sciences, Cairo University. The thin sections were investigated by a petrographic microscope, in order to determine textural attributes, pores, framework grains, cement morphology and micro-structures. The morphology and micro-structures of the cement were examined using SEM. The mineral composition was determined using powder X-ray diffraction (XRD). The CaCO<sub>3</sub> content was determined using pressure-calculator [38]. Stable isotopic values of oxygen and carbon ( $\delta^{18}\text{O}$  and  $\delta^{13}\text{C}$ ) of the carbonate cement were estimated for five samples using an automated carbonate preparation device (KIEL-III) coupled to a gas-ratio mass spectrometer (Finnigan MAT 252) at the Environmental Isotope Laboratory, Geosciences Department, University of Arizona. The cement was carefully separated using a micro-driller to avoid contamination. The cement was then reacted with dehydrated phosphoric acid under vacuum at 70 °C. The isotope ratio measurement is calibrated based on repeated measurements of NBS-19 and NBS-18, and precision is  $\pm 0.10\text{‰}$  for  $\delta^{18}\text{O}$  and  $\pm 0.08\text{‰}$  for  $\delta^{13}\text{C}$  (1 sigma).



**Figure 3.** Field Photographs showing the characteristic features and locations of the samples of the beachrock at the mouth of Wadi Al-Hamd. (a–c) The near horizontal to gently westward inclined gravel-rich proximal strata. (b) Close-up view of sample HMD1, showing normal grading from well-rounded gravel to massive sands. (d) Westward gently inclined graded bedded strata. (e) Fracture system in the distal beds. (f,g) Close-up view showing internal features of the poorly-sorted gravelly sand (HMD5) and the low angle cross bedded with foresets displaying normal grading in sample HMD 7.

#### 4. Results

Inland beachrocks are exposed at the mouth of Wadi Al-Hamd, South Al-Wajh, at about 1.1 km to the east of the recent shoreline, formed by an accumulation of coarse clastic sediments with a westward decrease in the grain size (Figure 3a–g). They occur at about a meter above the current sea-level and extend for about 60 m in N-S direction and up to 40 m in the E-W direction. They consist of 10 to 20 cm thick tabular beds of well-cemented terrigenous very coarse sands and gravels gently inclined ( $<10^\circ$ ) to the west (seaward) (Figure 3d). They vary with downdip in the grain size and internal sedimentary structures. Beds in the proximal part are sharp-based, mantled with poorly-sorted, well-rounded pebble-grade spherical to elongated, gravel-grade sand, and vertical to well-sorted sand (Figure 3b). In the distal location, beds vary from massive, parallel horizontal laminated and planar cross-stratified, with foresets defined by gravel concentration and displaying normal grading (Figure 3f). They are fractured orthogonally to the bedding plane (Figure 3e). Body and trace fossils are not recognized in the exposed rocks.

##### 4.1. Framework Composition and Cementation

The beachrocks of Wadi Al-Hamd cover a range of grain sizes, varying from generally poorly- to moderately-sorted sandy conglomerate to gravelly sandstones. Pebbles are rounded to subrounded and consist of lithic fragments, dominantly basalt and chert. Thin-section investigations showed that the framework composition consists mainly of siliclastic grains, dominated by mono- and polycrystalline quartz, feldspars, lithic fragments of quartzite, basalts, chert and rare limestones, amphiboles and rare heavy minerals rutile and tourmaline (Figure 4a–h). The siliclastic terrigenous grains are derived from rocks of the Hijaz and Midyan terranes and from the Quaternary limestones in the hinterland.

Skeletal remains (Figure 4b,d,f) are very rare (<2%) and dominated by algae, bivalves, echinoids, gastropods and larger benthic foraminifera. The skeletal remains were possibly transported by a longshore drift from offshore. The original porosity of the beachrocks was intergranular (and very rarely intragranular) and was totally to partially occluded by cementation and, locally, by internal sediments. The CaCO<sub>3</sub> content is generally low to moderate, varying from 28 to 53% with an average of 25% (Table 1).

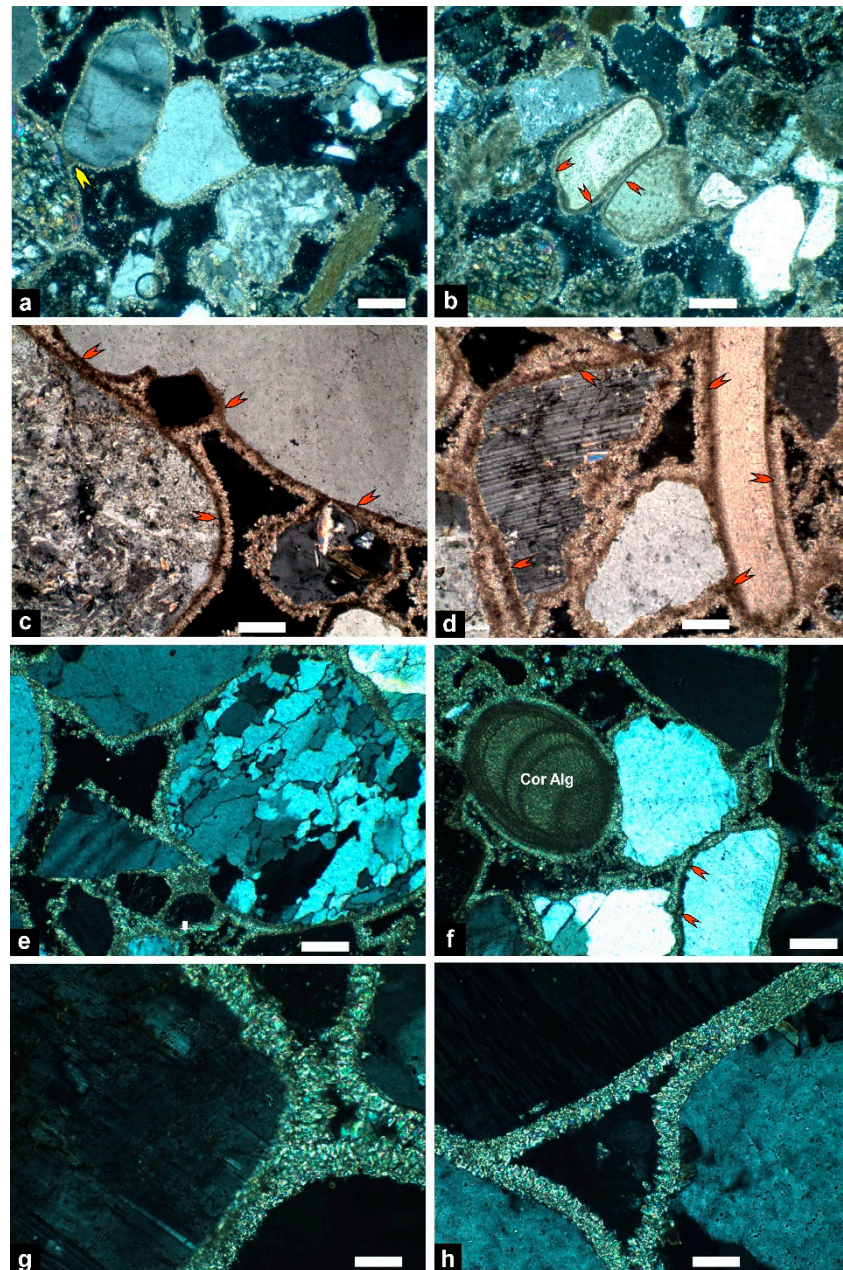


**Figure 4.** Photomicrographs showing the framework composition and the cement morphology in the Wadi Al-Hamd beachrocks. (a–c,f) The beachrock consists mainly of siliciclastic grains surrounded by isopachous Mg-calcite cement, a blade shape with a micritic base (red arrows). Pore-filling micrite taking a meniscus fabric is shown by yellow arrow in a. (a,b): sample HMD 1, (c): sample HMD 6, (d): sample HMD 7. (e,g,h) Samples HMD 2 and 5, showing the isopachous HMC cement that takes a blade shape without micritic base. (The bars in (a–f) = 200  $\mu$ m, and in (g) and (h) = 40  $\mu$ m).

**Table 1.** The oxygen and carbon stable isotope, Z values and CaCO<sub>3</sub> % content of the Wadi Al-Hamd beachrocks.

Sample	$\delta^{13}\text{C}_{\text{VPDB}}\text{‰}$	$\delta^{18}\text{O}_{\text{VPDB}}\text{‰}$	Z Values	CaCO <sub>3</sub> %
HMD 1	−0.09	−0.22	127	28
HMD 2	3.03	1.00	134	29
HMD 5	2.02	0.74	131.8	27
HMD 6	2.41	0.08	132.3	29
HMD 7	1.89	−0.35	131	53

The cement takes the form of isopachous and anisopachous bladed crystals up to 18.4  $\mu\text{m}$  surrounding grains, micrite envelope and pore filling microcrystalline cement (Figure 4a–h). Isopachous rims around the grains are non-selective, covering both siliciclastic and carbonate grains (Figure 4b–d). The cement lines grains or completely fills the intergranular pores (Figure 3g,h). Some grains are surrounded directly by isopachous blade crystals, and some display micritic base as a first generation of cement, followed by the bladed crystals. The crystals of the rims are arranged sub-perpendicularly to chaotically on the surface of siliciclastic grains (Figure 5a–h). SEM analysis shows that radial aggregate encrusting a previous, bladed cement is observed (Figure 5e). In addition, the micritic cement is associated in sample HMD 5 with filaments (Figure 5c,d). The cement consists mainly of high-Mg calcite, as revealed by XRD, petrographic and SEM investigations.

#### 4.2. Carbon and Oxygen Stable Isotopes

Carbon and oxygen stable isotopes are widely used to determine the origin of the water from which the cement is precipitated [39–41]. The overall  $\delta^{13}\text{C}_{\text{VPDB}}$  values of the cement vary between  $-1.09\text{‰}$  to  $3.03\text{‰}$  (mean  $1.85\text{‰}$ ), and the  $\delta^{18}\text{O}_{\text{VPDB}}$  values range from  $-0.35\text{‰}$  to  $1.00\text{‰}$  (mean  $0.25\text{‰}$ ) (Table 1). Only the cement of the most proximal sample (HMD1) is depleted in oxygen and carbon isotopic values ( $-0.09$  and  $-0.22\text{‰}$ , respectively). However, the average  $\delta^{13}\text{C}_{\text{VPDB}}$  and  $\delta^{18}\text{O}_{\text{VPDB}}$  values are higher than the limit established for modern marine carbonates ( $\delta^{13}\text{C}_{\text{VPDB}}$ ;  $-2.00\text{‰}$ ) and modern seawater ( $\delta^{18}\text{O}_{\text{VPDB}}$ ;  $-4.00\text{‰}$ ) [42].

The  $\delta^{18}\text{O}$  values of the cements of the Wadi Al-Hamd beachrocks are slightly lighter isotopically than those recorded from the Egyptian Red Sea and Mediterranean beachrocks [19]. The  $\delta^{18}\text{O}$  and  $\delta^{13}\text{C}$  values of the Mediterranean beachrock cements range between  $-0.40$  and  $+1.20\text{‰}$  (mean of  $+0.50\text{‰}$ ) and  $+1.00$  to  $+2.10$ , respectively. On the other hand, the  $\delta^{18}\text{O}$  and  $\delta^{13}\text{C}$  values of the Red Sea beachrock cements range between  $-0.10$  and  $+1.20$  (mean of  $+0.50\text{‰}$ ) and from  $+2.10$  to  $4.50\text{‰}$ , respectively [19]. Therefore, it appears that the mean values of oxygen and carbon isotopic compositions are relatively identical for the cements of both localities (Figure 6).

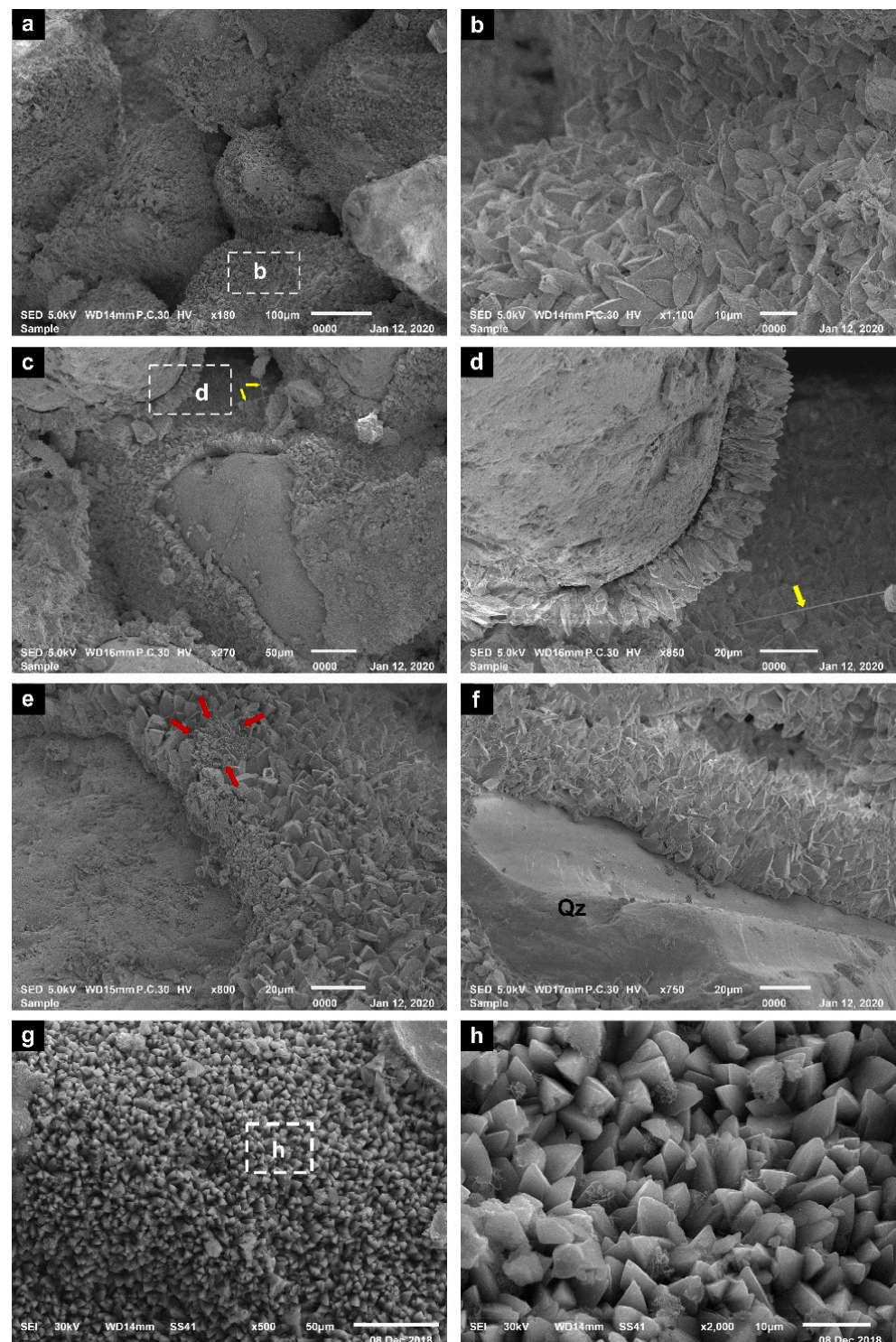


**Figure 5.** SEM photo micrographs showing the characteristic features of the carbonate cement in the Wadi Al-Hamd beachrocks. **(a,b)** HMC blades surrounding grains and the crystals show random orientation (sample HMD 1). **(c–e)** Isopachous HMC calcite blades grow perpendicular to the grain surface (sample HMD 5). The length of the blades is up to 18.3  $\mu\text{m}$ ; note the organic filaments (yellow arrows) that support the contribution of algal activity in cement formation. Small radial aggregate encrusting the bladed cement is shown by red arrows. **(f–h)** Pore-filling HMC calcite cements taking a well-developed bladed shape (sample HMD 7) surrounding quartz (Qz).

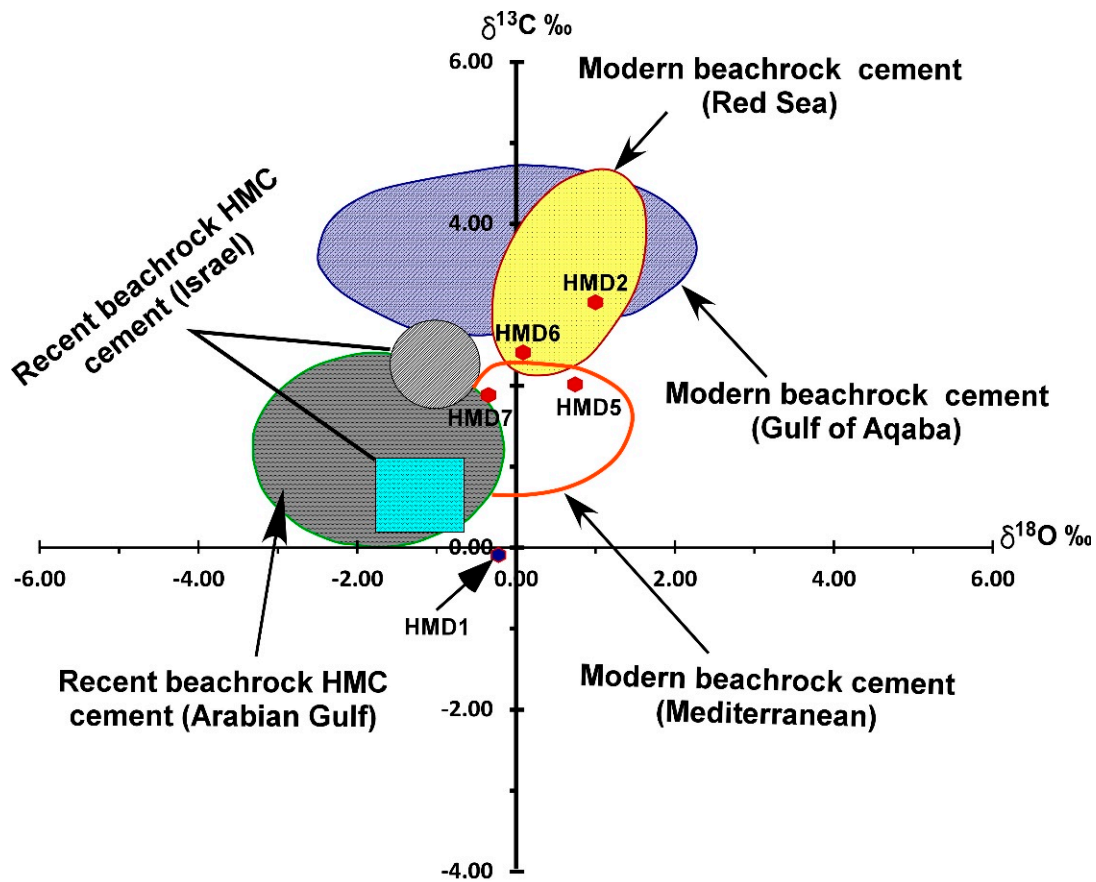


**Figure 6.** Bivariate plot between carbon and oxygen stable isotope composition of the Wadi Al-Hamd beachrocks and other beachrocks in the Arabian and Aqaba gulfs [32], Bahamian beachrocks [43], Red Sea and Mediterranean Sea [19], Mediterranean beachrocks of Israel [42].

The Z value [44] is determined to distinguish the type of porewater from which the carbonate cement is precipitated. The Z value is calculated as follows:

$$Z = a(\delta^{13}\text{C} + 50) + b(\delta^{18}\text{O} + 50)$$

where a and b are constants values equal 2.048 and 0.498, respectively. Z values > 120 indicate a cement of marine-water origin, whereas values < 120 suggest a freshwater origin. The Z values obtained for the studied samples, ranging from 127.003 to 134.006‰ (average; 131.22‰), suggest that the cement was generally generated by a dominantly marine origin.

### 5. Discussion

The grain size, sedimentary structures, framework composition and cement composition and fabric of the Wadi Al-Hamd beachrocks provide information of the climate and sea level changes surrounding it. The data indicate that the climate was more humid during the deposition of the sediments constituting the beachrock, and the sea level was higher than its present position. The prevalence of siliclastic coarse sediments in the beachrocks suggests a period of active wadi discharge. The low content of CaCO<sub>3</sub> reflects the dominance of siliclastic terrigenous constituents. The CaCO<sub>3</sub> content is attributed to the carbonate cement and rare calcareous skeletal remains. Active wadi discharge is related to a humid climate with relatively high rates of precipitation. In general, coarse clastic sediments are remarkably absent or constitute only a minor proportion of the modern Red Sea nearshore sediments [45]. Most wadis (the main conduit of terrigenous sediments) disappear halfway into the Red Sea coast, and very little fine-grained terrigenous sediments arrive to the nearshore zone because of the extreme aridity. The modern unconsolidated

beach and nearshore sediments consist mainly of fine- to medium-grained sands [46]. Similarly, the shallow subsurface sediments of the wadi mouth and nearshore environments are dominantly medium- and, rarely, coarse-grained sands [47], finer than that of beachrocks. The gravel-rich beachrocks at the mouth of Wadi Al-Hamd were transported, therefore, and deposited by a greater runoff, under a much more humid climate than what prevails today. This humid interval possibly coincides with the middle Holocene pluvial period [45]. Several examples have been reported from inland basins and Red Sea coastal zones in western Saudi Arabia, suggesting a middle Holocene long-term climatic humid climate ([6,9,45,48]. The carbon and oxygen isotopic data of the Gulf of Aqaba fossil corals suggest that the climate of the area was humid prior to 4.9 ka ago, and that after that, the climate turned extremely arid [49]. Evidence for regional aridity starting about 5 ka has been reported [3]. The gravel and medium- to coarse-grained sands containing rare skeletal remains suggest deposition in a relatively higher energy environment. The occurrence of skeletal remains suggests a marine-influenced environment. The horizontal to gently seaward inclined beds, displaying horizontal to planar cross lamination, suggest deposition under variable energy conditions within the beach (upper foreshore) environment [50].

The area of study is situated in a tectonically stable zone [51], which extends from the north of Al-Wajh City (~N 26°) to the north of the Al-Quattan (~N 21°). The occurrence of the beachrocks 1.1 km inland suggests that the sea level must have maintained such a high position for some time to allow deposition of the coarse sediments. Therefore, during the deposition of beachrocks the Red Sea coastal plain at the mouth of Wadi Al-Hamd was flooded during a period of relative sea level rise, and the shoreline migrated farther inland. The beachrocks under investigation are permanently emergent above the present high tide level. This may indicate that the sea level during deposition of the beachrock sediments was 1.3 m, or slightly higher than the current sea level. Along the Red Sea coastline, a mid-Holocene sea level highstand with high spatial and temporal variability is observed [51,52]. A sea level up to a maximum of 1–2 m higher than the present was recorded for the mid-Holocene [51,53].

#### *Cementation Patterns*

Petrographic examination and the isotopic values of the cement suggest that cementation took place in the intertidal environment under marine conditions, and there is no evidence for cementation within the meteoric environment. The beach setting is ideal for the precipitation of abiotic marine cements. High energy conditions, including wave and tidal activity, and relatively coarse, highly porous and permeable sediments, ensure that adequate volumes of supersaturated marine water are able to move through the pore system to enable cementation with the aid of hot weather. Interestingly, the samples had similar cements, indicating that the same processes of cementation occurred.

Clasts cemented with HMC bladed cement indicate cementation in an intertidal zone under active marine phreatic conditions [54–56]. Similar cement types were reported from the Mediterranean and Bermuda beachrocks, and were interpreted as a product of marine cementation [57]. The micrite HMC cement, with local occurrence of organic filaments in the studied beachrocks, may be related to biological activity. The role of micro-organisms in the formation of micrite cement has been reported by several authors [25,58]. Micritic pore-fillings suggest the involvement of biological activity [55]. In cases of no relict cellular or laminar structures, micrite cement indicates rapid supersaturation of pore waters and multiple instances of nucleation [55]. The grain-to-grain meniscal bridges following micrite encrustations imply vadose conditions [58,59].

Based on the isotopic data, it is apparent that cementation took place within the marine beach environment. The isotopic values of the cement show mostly positive carbon and oxygen values. The negative  $\delta^{13}\text{C}_{\text{VPDB}}$  and  $\delta^{18}\text{O}_{\text{VPDB}}$  values from the most proximal sample (HMD1) may indicate the possible contribution of fresh water in the cement precipitation. The depletion in  $\delta^{18}\text{O}$  and  $\delta^{13}\text{C}$  isotopic values of beachrock carbonate cements from Brazil and the Canary Islands (Spain) were attributed to the slight modification by meteoric water

at relatively low salinity and at relatively high temperatures [60–62]. The limited isotopic heterogeneity among samples suggests a stability of water composition and temperature during the cement formation [19,62]. Isotopic values of most samples plot within the modern marine beachrock cement field of the Red Sea, Mediterranean Sea, Gulf of Aqaba and straddle Arabian Gulf field [19,32,42]. The high-Mg calcites both the Arabian and the Aqaba Gulfs possess relatively depleted  $\delta^{13}\text{C}$  values than those of the cement of the Wadi Al-Hamd beachrocks. High-Mg calcite precipitated in the present day under warm shallow seawater is relatively enriched in oxygen (+3.00 ‰) and carbon ( $+3.5 \pm 1.5$  ‰) isotopic values [23,63]. The  $\delta^{18}\text{O}$  (−0.35 to +1.00 ‰) and the  $\delta^{13}\text{C}$  (−0.09 to +3.03 ‰) values of the high-Mg calcite cement of the Wadi Al-Hamd beachrocks indicate precipitation in equilibrium with present-day seawater. A value of 0.54 ‰  $\delta^{18}\text{O}$  indicates cementation in the intertidal zone [64].

## 6. Conclusions

An interesting beachrock is exposed 1.1 km inland at the Red Sea coastal plain at the mouth of Wadi Al-Hamd. It bears criteria that can be used to interpret Holocene climate and sea level changes. The following concluding remarks are:

1. The grain size, sedimentary structures and framework compositions indicate that the sediments were derived during humid intervals mainly from a terrigenous source, with little contribution of marine derived calcareous skeletal remains. They were deposited in a high-energy beach environment.
2. Deposition in the beach environment suggests that the shoreline backstepped more landward during a period of relative sea level rise. The beachrock at the mouth of Wadi Al-Hamd is therefore a paleoshoreline indicator.
3. The suggested humid climate and relative sea level highstand may be correlated with the middle Holocene humid interval and sea level highstand.
4. The dominant isopachous bladed and micritic Mg-calcite cement suggests that cement growth in the intertidal zone under active marine phreatic conditions. This is supported by the isotopic data and Z values that indicate that the cement generally originated from marine water. The meniscus fabric and the depletion of oxygen and carbon isotope values in the most proximal sample may suggest a slight contribution from meteoric water in the vadose environment.

**Author Contributions:** All authors contributed to every stage of the work. Conceptualization, fieldwork and data collection were done by all authors. The microscopic investigations, data analysis and first draft of the manuscript was written by I.M.G., A.A.M. and R.A.H. Reviewed and commented on early versions of the manuscript written by I.M.G. Project administration and funding acquisition were under the supervision of A.A.M. All authors have read and agreed to the published version of the manuscript.

**Funding:** This project was funded by the Deanship of Scientific Research (DSR) at King Abdulaziz University, Jeddah, Grant No. G22-150-1439.

**Institutional Review Board Statement:** Not applicable.

**Informed Consent Statement:** Not applicable.

**Data Availability Statement:** Not applicable.

**Acknowledgments:** This project was funded by the Deanship of Scientific Research (DSR) at King Abdulaziz University, Jeddah, under Grant No. G22-150-1439. The authors thank the DSR for this technical and financial support. The authors thank Aaid Al-Zubeiri and Bandar El-Zahrani (KAU) for their assistance during field studies and sample collection. We are very grateful to the editor and the reviewers for their constructive comments and editorial handling.

**Conflicts of Interest:** The authors declare no conflict of interest.

## References

1. Vacchi, M.; Marriner, N.; Morhange, C.; Spada, G.; Fontana, A.; Rovere, A. Multiproxy assessment of Holocene relative sea-level changes in the western Mediterranean: Sea-level variability and improvements in the definition of the isostatic signal. *Earth-Sci. Rev.* **2016**, *155*, 172–197. [[CrossRef](#)]
2. Nakada, M.; Kimura, R.; Okuno, J.; Moriwaki, K.; Miura, H.; Maemoku, H. Late Pleistocene and Holocene melting history of the Antarctic ice sheet derived from sea-level variations. *Mar. Geol.* **2000**, *167*, 85–103. [[CrossRef](#)]
3. Demenocal, P.; Ortiz, J.; Guilderson, T.; Adkins, J.; Sarnthein, M.; Baker, L.; Yarusinsky, M. Abrupt onset and termination of the African Humid Period: Rapid climate responses to gradual insolation forcing. *Quat. Sci. Rev.* **2000**, *19*, 347–361. [[CrossRef](#)]
4. Hein, C.J.; FitzGerald, D.M.; Milne, G.A.; Bard, K.; Fattovich, R. Evolution of a Pharaonic harbor on the Red Sea: Implications for coastal response to changes in sea level and climate. *Geology* **2011**, *39*, 687–690. [[CrossRef](#)]
5. Ghandour, I.M.; Al-Washmi, H.A.; Haredy, R.A.; Al-Zubieri, A.G. Facies evolution and depositional model of an arid microtidal coast: Example from the coastal plain at the mouth of Wadi Al-Hamd, Red Sea, Saudi Arabia. *Turk. J. Earth Sci.* **2016**, *25*, 256–273. [[CrossRef](#)]
6. Ghandour, I.M.; Al-Zubieri, A.G.; Basaham, A.S.; Mannaa, A.A.; Al-Dubai, T.A.; Jones, B.G. Mid-Late Holocene Paleoenvironmental and Sea Level Reconstruction on the Al Lith Red Sea Coast, Saudi Arabia. *Front. Mar. Sci.* **2021**. [[CrossRef](#)]
7. Ghandour, I.M.; Haredy, R.A. Facies analysis and sequence stratigraphy of Al-Kharrar lagoon coastal sediments, Rabigh Area, Saudi Arabia: Impact of sea-level and climate changes on coastal evolution. *Arab. J. Sci. Eng.* **2019**, *44*, 505–520. [[CrossRef](#)]
8. Abu-Zied, R.H.; Bantan, R.A. Palaeoenvironment, palaeoclimate and sea-level changes in the Shuaiba Lagoon during the late Holocene (last 3.6 ka), eastern Red Sea coast, Saudi Arabia. *Holocene* **2015**, *25*, 1301–1312. [[CrossRef](#)]
9. Bantan, R.A.; Abu-Zied, R.H.; Al-Dubai, T.A. Late Holocene environmental changes in a sediment core from Al-Kharrar Lagoon, eastern Red Sea Coast, Saudi Arabia. *Arab. J. Sci. Eng.* **2019**, *44*, 6557–6570. [[CrossRef](#)]
10. Dickinson, W.R. Paleoshoreline record of relative Holocene sea levels on Pacific islands. *Earth-Sci. Rev.* **2001**, *55*, 191–234. [[CrossRef](#)]
11. Shaked, Y.; Marco, S.; Lazar, B.; Stein, M.; Cohen, C.; Sass, E.; Agnon, A. Late Holocene shorelines at the Gulf of Aqaba: Migrating shorelines under conditions of tectonic and sea level stability. *EGU Stephan Mueller Spec. Publ. Ser.* **2002**, *2*, 105–111. [[CrossRef](#)]
12. de Oliveira Caldas, L.H.; Stattegger, K.; Vital, H. Holocene sea-level history: Evidence from coastal sediments of the northern Rio Grande do Norte coast, NE Brazil. *Mar. Geol.* **2006**, *228*, 39–53. [[CrossRef](#)]
13. Mauz, B.; Vacchi, M.; Green, A.; Hoffmann, G.; Cooper, A. Beachrock: A tool for re-constructing relative sea level in the far-field. *Mar. Geol.* **2015**, *362*, 1–6. [[CrossRef](#)]
14. Manaa, A.A.; Jones, B.G.; McGregor, H.V.; Zhao, J.X.; Price, D.M. Dating Quaternary raised coral terraces along the Saudi Arabian Red Sea coast. *Mar. Geol.* **2016**, *374*, 59–72. [[CrossRef](#)]
15. Kelletat, D. Beachrock as sea-level indicator? Remarks from a geomorphological point of view. *J. Coast. Res.* **2006**, *22*, 1558–1564. [[CrossRef](#)]
16. Ozturk, M.Z.; Erginal, A.E.; Kiyak, N.G.; Ozturk, T. Cement fabrics and optical luminescence ages of beachrock, North Cyprus: Implications for Holocene sea-level changes. *Quat. Int.* **2016**, *401*, 132–140. [[CrossRef](#)]
17. Karkani, A.; Evelpidou, N.; Vacchi, M.; Morhange, C.; Tsukamoto, S.; Frechen, M.; Maroukian, H. Tracking shoreline evolution in central Cyclades (Greece) using beachrocks. *Mar. Geol.* **2017**, *388*, 25–37. [[CrossRef](#)]
18. Falkenroth, M.; Schneider, B.; Hoffmann, G. Beachrock as sea-level indicator—a case study at the coastline of Oman (Indian Ocean). *Quat. Sci. Rev.* **2019**, *206*, 81–98. [[CrossRef](#)]
19. Holail, H.; Rashed, M. Stable isotopic composition of carbonate-cemented recent beachrock along the Mediterranean and the Red Sea coasts of Egypt. *Mar. Geol.* **1992**, *106*, 141–148. [[CrossRef](#)]
20. Voudoukas, M.I.; Velegrakis, A.F.; Plomaritis, T.A. Beachrock occurrence, characteristics, formation mechanisms and impacts. *Earth-Sci. Rev.* **2007**, *85*, 23–46. [[CrossRef](#)]
21. Erginal, A.E.; Güneç, N.K.; Bozcu, M.; Ertek, A.; Güngüneş, H.; Sungur, A.; Türker, G. On the origin and age of the Anıburnu beachrock, Gelibolu Peninsula, Turkey. *Turk. J. Earth Sci.* **2008**, *17*, 803–819.
22. Ghandour, I.M.; Al-Washmi, H.A.; Bantan, R.A.; Gadallah, M.M. Petrographical and petrophysical characteristics of asynchronous beachrocks along Al-Shoaiba Coast, Red Sea, Saudi Arabia. *Arab. J. Geosci.* **2014**, *7*, 355–365. [[CrossRef](#)]
23. Milliman, J.D. *Recent Sedimentary Carbonates: Part 1 Marine Carbonates*; Springer: New York, NY, USA, 1974; p. 375.
24. Hanor, J.S. Precipitation of beachrock cements; mixing of marine and meteoric waters vs. CO<sub>2</sub>-degassing. *J. Sediment. Res.* **1978**, *48*, 489–501.
25. Neumeier, U. Experimental modelling of beachrock cementation under microbial influence. *Sediment. Geol.* **1999**, *126*, 35–46. [[CrossRef](#)]
26. El-Shater, A.; Abu Ouf, M.A. Beachrock in South Jeddah, The Red Sea Coast of Saudi Arabia. *J. King Abdulaziz Univ. Mar. Sci.* **1995**, *6*, 53–65. [[CrossRef](#)]
27. Al-Ramadan, K. Diagenesis of Holocene beachrocks: A comparative study between the Arabian Gulf and the Gulf of Aqaba, Saudi Arabia. *Arab. J. Geosci.* **2014**, *7*, 4933–4942. [[CrossRef](#)]
28. Koeshidayatullah, A.; Al-Ramadan, K. Unraveling cementation environment and patterns of Holocene beachrocks in the Arabian Gulf and the Gulf of Aqaba: Stable isotope approach. *Geol. Q.* **2014**, *58*, 207–216. [[CrossRef](#)]
29. Haredy, R.A.; Ghandour, I.M.; Erginal, A.E.; Bozcu, M. Beachrock Cementation Patterns Along the Gulf of Aqaba Coast, Saudi Arabia. *Arab. J. Sci. Eng.* **2019**, *44*, 479–487. [[CrossRef](#)]

30. Strasser, A.; Strohmenger, C.; Davaud, E.; Bach, A. Sequential evolution and diagenesis of Pleistocene coral reefs (South Sinai, Egypt). *Sediment. Geol.* **1992**, *78*, 59–79. [[CrossRef](#)]
31. Strasser, A.; Strohmenger, C. Early diagenesis in Pleistocene coral reefs, southern Sinai, Egypt: Response to tectonics, sea-level and climate. *Sedimentology* **1997**, *44*, 537–558. [[CrossRef](#)]
32. Holail, H.M.; Shaaban, M.N.; Mansour, A.S. Cementation of Holocene beachrock in the Aqaba and the Arabian Gulfs: Comparative study. *Carbonates Evaporites* **2004**, *19*, 142–150. [[CrossRef](#)]
33. Morcos, S.A. Physical and chemical oceanography of the Red Sea. *Oceanogr. Mar. Biol. Annu. Rev.* **1970**, *8*, 73–202.
34. Ghandour, I.M.; Al-Washmi, H.A.; Haredy, R.A. Gravel-sized mud clasts on an arid microtidal sandy beach: Example from the northeastern Red Sea, South Al-Wajh, Saudi Arabia. *J. Coast. Res.* **2013**, *29*, 110–117. [[CrossRef](#)]
35. Bantan, R.A.; Ghandour, I.M.; Al-Zubieri, A.G. Mineralogical and geochemical composition of the subsurface sediments at the mouth of Wadi Al-Hamd, Red Sea coast, Saudi Arabia: Implication for provenance and climate. *Environ. Earth Sci.* **2020**, *79*, 1–20. [[CrossRef](#)]
36. Moufti, A.M. Mineralogy and mineral chemistry of auriferous stream sediments from Al Wajh area, NW Saudi Arabia. *Arab. J. Geosci.* **2009**, *2*, 1–17. [[CrossRef](#)]
37. Davies, F.B. *Explanatory Notes on the Geologic Map of Al Wajh Quadrangle, Sheet 26 B*; Ministry of Petroleum and Mineral Resources, Deputy Ministry for Mineral Resources: Jeddah, Saudi Arabia, 1985; p. 27.
38. Sherrod, L.A.; Dunn, G.; Peterson, G.A.; Kolberg, R.L. Inorganic carbon analysis by modified pressure-calimeter method. *Soil Sci. Soc. Am. J.* **2002**, *66*, 299–305. [[CrossRef](#)]
39. Allan, J.R.; Matthews, R.K. Isotope signatures associated with early meteoric diagenesis. *Sedimentology* **1982**, *29*, 797–817. [[CrossRef](#)]
40. Spurgeon, D.; Davis, R.A., Jr.; Shinnu, E.A. Formation of Beach Rock at Siesta Key, Florida and its influence on barrier island development. *Mar. Geol.* **2003**, *200*, 19–29. [[CrossRef](#)]
41. Armstrong-Altrin, J.S.; Lee, Y.I.; Verma, S.P.; Worden, R.H. Carbon, oxygen, and strontium isotope geochemistry of carbonate rocks of the upper Miocene Kudankulam Formation, southern India: Implications for paleoenvironment and diagenesis. *Geochemistry* **2009**, *69*, 45–60. [[CrossRef](#)]
42. Magaritz, M.; Gavish, E.; Bakler, N.; Kafri, U. Carbon and oxygen isotope composition-indicators of cementation environment in Recent, Holocene and Pleistocene sediments along the coast of Israel. *J. Sediment. Petrol.* **1979**, *49*, 401–411.
43. Beier, J.A. Diagenesis of Quaternary Bahamian beachrock; petrographic and isotopic evidence. *J. Sediment. Res.* **1985**, *55*, 755–761. [[CrossRef](#)]
44. Keith, M.L.; Weber, J.N. Carbon and oxygen isotopic composition of selected limestones and fossils. *Geochim. et Cosmochim. Acta* **1964**, *28*, 1787–1816. [[CrossRef](#)]
45. Rao, N.D.; Behairy, A.K. Intertidal conglomerate south of Yanbu-An episodic clastic deposit in the eastern Red Sea. *Palaeogeogr. Palaeoclimatol. Palaeoecol.* **1987**, *58*, 221–228.
46. Ghandour, I.M. Controlling factors on the textural characteristics of the coastal sediments around Wadi Al-Hamd mouth Delta, NE Red Sea, Saudi Arabia. *J. King Abdulaziz Univ. Mar. Sci.* **2014**, *25*, 61–78. [[CrossRef](#)]
47. Al-Zubieri, A.G.; Ghandour, I.M.; Haredy, R.A. Controlling factors on the grain size distribution of shallow subsurface coastal sediments at the mouth of Wadi Al-Hamd, northeastern Red Sea, Saudi Arabia. *J. King Abdulaziz Univ. Mar. Sci.* **2018**, *27*, 1–17.
48. Jado, A.R.; Zötl, J.G. *Quaternary period in Saudi Arabia*; Springer: Wien, Austria, 1984; p. 360.
49. Moustafa, Y.A.; Pätzold, J.; Loya, Y.; Wefer, G. Mid-Holocene stable isotope record of corals from the northern Red Sea. *Int. J. Earth Sci.* **2000**, *88*, 742–751. [[CrossRef](#)]
50. Clifton, H.E. Progradational sequences in Miocene shoreline deposits, southeastern Caliente Range, California. *J. Sediment. Res.* **1981**, *51*, 165–184.
51. Khanna, P.; Petrovic, A.; Ramdani, A.I.; Homewood, P.; Mettraux, M.; Vahrenkamp, V. Mid-Holocene to present circum-Arabian sea level database: Investigating future coastal ocean inundation risk along the Arabian plate shorelines. *Quat. Sci. Rev.* **2021**, *261*, 106959. [[CrossRef](#)]
52. Al-Mikhlaifi, A.S.; Hibbert, F.D.; Edwards, L.R.; Cheng, H. Holocene relative sea-level changes and coastal evolution along the coastlines of Kamaran Island and As-Salif Pen-insula, Yemen, southern Red Sea. *Quat. Sci. Rev.* **2021**, *252*, 106719. [[CrossRef](#)]
53. Murray-Wallace, C.V.; Woodroffe, C.D. *Quaternary Sea-Level Changes: A Global Perspective*; Cambridge University Press: New York, NY, USA, 2014; p. 484.
54. James, N.P.; Choquette, P.W. Limestone: The sea floor diagenetic environment. In *Diagenesis*; McIlreath, I., Morrow, D., Eds.; Geological Association of Canada Reprint Series: St John's, ND, Canada, 1990; pp. 13–34.
55. Vieira, M.M.; De Ros, L.F. Cementation patterns and genetic implications of Holocene beachrocks from northeastern Brazil. *Sediment. Geol.* **2006**, *192*, 207–230. [[CrossRef](#)]
56. Desruelles, S.; Fouache, É.; Ciner, A.; Dalongeville, R.; Pavlopoulos, K.; Kosun, E.; Coquinot, Y.; Potdevin, J.L. Beachrocks and sea level changes since Middle Holocene: Comparison between the insular group of Mykonos–Delos–Rhenia (Cyclades, Greece) and the southern coast of Turkey. *Glob. Planet. Chang.* **2009**, *66*, 19–33. [[CrossRef](#)]
57. Alexanderson, T. Mediterranean beachrock cementation: Marine precipitation of Mg-calcite. In *The Mediterranean Sea: A Natural Sedimentation Laboratory*; Stanley, D.J., Ed.; Dowden, Hutchinson and Ross Publishers: Stroudsburg, PA, USA, 1972; pp. 203–223.
58. Strasser, A.; Davaud, E.; Jedoui, Y. Carbonate cements in Holocene beachrock: Example from Bahiret et Biban, southeastern Tunisia. *Sediment. Geol.* **1989**, *62*, 89–100. [[CrossRef](#)]

59. Meyers, J.H. Marine vadose beachrock cementation by cryptocrystalline magnesian cal-cite, Maui, Hawaii. *J. Sediment. Res.* **1987**, *57*, 558–570.
60. Chaves, N.S.; Sial, A.N. Mixed oceanic and freshwater depositional conditions for beachrocks of Northeast Brazil: Evidence from carbon and oxygen isotopes. *Int. Geol. Rev.* **1998**, *40*, 748–754. [[CrossRef](#)]
61. Calvet, F.; Cabrera, M.C.; Carracedo, J.C.; Mangas, J.; Pérez-Torrado, F.J.; Recio, C.; Travé, A. Beachrocks from the island of La Palma (Canary Islands, Spain). *Mar. Geol.* **2003**, *197*, 75–93. [[CrossRef](#)]
62. Vieira, M.M.; Sial, A.N.; De Ros, L.F.; Morad, S. Origin of Holocene beachrock cements in northeastern Brazil: Evidence from carbon and oxygen isotopes. *J. South Am. Earth Sci.* **2017**, *79*, 401–408. [[CrossRef](#)]
63. Hudson, J.D. Stable isotopes of limestone lithification. *J. Geol. Soc. Lond.* **1977**, *133*, 637–660. [[CrossRef](#)]
64. Coudray, J.; Montaggioni, L. The diagenetic products of marine carbonate as sea level indicators. In *Sea-Level Research: A Manual for the Collection and Evaluation of Data*; Plassche, O.V.D., Ed.; Geo Books: Norwich, UK, 1986; pp. 311–360.